Collective excitations in open-shell metal clusters: The time-dependent local-density approximation applied to the self-consistent spheroidal jellium particle

W. Ekardt and Z. Penzar*
Fritz-Haber-Institut der Max-Planck-Gesellschaft, Faradayweg 4-6, D-1000 Berlin 33, Germany
(Received 21 December 1989; revised manuscript received 15 June 1990)

The self-consistent and microscopic time-dependent local-density-approximation (TDLDA) formalism for the calculation of the dynamical electronic response properties of open-shell, axially deformed small metal clusters is presented in detail. The model is based on the self-consistent ground-state calculation of the spheroidal jellium model, giving the optimized cluster shape, driven by its open-valence-shell electronic structure. First results on the static and dynamical electronic polarizability of the strongly axially deformed Na_{10} cluster are reported and compared with the experimental polarizability and photoabsorption cross-section results. The variety of the future applications of the model is outlined, as well as the possible improvement of the formalism.

I. INTRODUCTION

The self-consistent spherical jellium model[1-6] for the description of the electronic properties mainly of the *sp*-bonded metals such as Li,Na,K, and for the noble metals Cu,Ag,Au was extended by us recently[7] to improve the jellium description of those clusters, whose electronic shells are—within the spherical description—not completely filled. First results of this study were published in Ref. 7 for some ground-state properties like abundances and ionization potentials. In the present work we investigate such dynamical properties as the excitation of plasmons or single electron-hole pairs within a method that was previously applied to spherical jellium clusters by one of us.[8,9] In the spherical case the problem is relatively simple because the angular momentum of the external field is preserved [that is, for a *dipole* perturbation ($l=1$) we obtain a *dipole* answer ($l=1$)]. However, in the *spheroidal* problem the only preserved quantum numbers are the parity p and the azimuthal quantum number m. Hence the problem is much more difficult than in the spherical case ($l=1$ couples to e.g., $l=1$, $l=3$, $l=5$, etc.) and the calculation is much more demanding. Of course the result depends on the relative orientation of the external field and the symmetry axis of the spheroid, which results in the splitting of the spherical plasmon line. As one might expect, the present TDLDA (Refs. 8 and 9) (time-dependent local-density approximation) calculation has the same intrinsic flaws as the corresponding spherical theory:[8,9] The static polarizabilities are too low by about 20% and the dynamical excitation frequencies too high by about 10–15 %, when compared with experiment. Furthermore, the linewidth as determined by the pure TDLDA does not agree with the experimental data. As discussed recently by Pacheco and Broglia,[10] this width is to be calculated from the coupling of shape fluctuations to the plasmon.[11] These points will be further addressed in the text.

II. THEORY

As the response formalism relies heavily on some properties of the Kohn-Sham equations[8,9] in spheroidal coordinates,[12] we give in the following a few details with regard to the solution of these equations. In our theory, we model the positive ionic background by a rotational spheroid.[7] The rotational spheroid is formed by rotating an ellipse around one of its principal axes. It possesses rotational symmetry around the z axis and is symmetric with respect to reflection in the midplane.[13] Because of the approximate spheroidal geometry of the ensuing Kohn-Sham potential, we chose to determine the Kohn-Sham orbitals $\psi_i(\xi,\eta,\phi)$ and their corresponding energy eigenvalues ε_i from the Kohn-Sham equations in spheroidal coordinates[13,14]

$$\left\{-\frac{1}{2}\left[\frac{\partial}{\partial\xi}(\xi^2-1)\frac{\partial}{\partial\xi}+\frac{\partial}{\partial\eta}(1-\eta^2)\frac{\partial}{\partial\eta}+\left[\frac{1}{\xi^2-1}+\frac{1}{1-\eta^2}\right]\frac{\partial^2}{\partial\phi^2}\right]+a^2(\xi^2-\eta^2)V^{\text{eff}}(\xi,\eta)-a^2(\xi^2-\eta^2)\varepsilon_i\right\}\psi_i(\xi,\eta,\phi)=0\ . \quad (1)$$

Here, ξ is the "radial" and η,ϕ are the angular spheroidal coordinates.[13] Furthermore, one-half of the interfocal distance is denoted by

$$a=|z_0^2-\rho_0^2|^{1/2}\ , \quad (2)$$

where z_0 and ρ_0 are the principal axes of the ellipse, generating the jellium spheroid and the accompanying spheroidal coordinate system.

In Eq. (1) V^{eff} is the Kohn-Sham potential to be determined self-consistently.[1,12] In accordance with the as-

sumption of rotational invariance of the positive jellium background around the z axis, the resulting electronic particle density distribution, $n_-(\mathbf{r})$, is rotationally averaged around the same axis. This leads to the independence of V^{eff} on the azimuthal coordinate ϕ, and hence only to its dependence of ξ,η, as denoted in Eq. (1).

In contrast to the much simpler case of spherically symmetric potentials,[1] the wave functions now contain *more* than one angular component l,

$$\psi_i(\xi,\eta,\phi)=\sum_i X_l^{m,p}(\xi;\varepsilon_i)Y_l^m(\eta;\phi), \quad i\equiv(m,p,n) \tag{3}$$

where

$$l=\begin{cases}|m|+2k, & p=+\\ |m|+2k+1, & p=-;\quad m=0,\pm1,\pm2,\ldots,\end{cases}$$
$$k=0,1,2,\ldots,\ n=1,2,3,\ldots . \tag{4}$$

Here $Y_l^m(\eta;\phi)$ are ordinary spherical harmonics, p is the parity (with respect to reflection at the mid-plane of the spheroid; $p=\pm$), and m is the projection of the angular momentum on the z axis. Due to the assumed symmetry of the problem, p and m are the only two conserved quantum numbers, related to symmetry. The state ψ_i $[i\equiv(m,p,n)]$ in Eq. (3) is the state of symmetry (m,p) with the nth lowest energy eigenvalue.

Making use of the expansion (3), after multiplying Eq. (1) by $Y_{l'}^{*m}(\eta,\phi)$ and integrating it over $\int_0^{2\pi}d\phi\int_{-1}^{1}d\eta$, we obtain the system of coupled differential equations for the components $X_l^{m,p}(\xi;\varepsilon_i)$,

$$\sum_l\left[-\frac{1}{2}\left[\frac{d}{d\xi}(\xi^2-1)\frac{d}{d\xi}-l(l+1)-\frac{m^2}{\xi^2-1}\right]\delta_{l',l}+[V^{\text{eff}}]^m_{l',l}(a,\xi)-\varepsilon_i D^m_{l',l}(a,\xi)\right]X_l^{m,p}(\xi;\varepsilon_i)=0 . \tag{5}$$

Here we denoted

$$D^m_{l',l}(a,\xi)=\int_0^{2\pi}d\phi\int_{-1}^{1}d\eta\, Y_{l'}^{*m}(\eta,\phi)\times[a^2(\xi^2-\eta^2)]Y_l^m(\eta,\phi) \tag{6}$$

and

$$[V^{\text{eff}}]^m_{l',l}(a,\xi)=\int_0^{2\pi}d\phi\int_{-1}^{1}d\eta\, Y_{l'}^{*m}(\eta,\phi)[a^2(\xi^2-\eta^2)]\times V^{\text{eff}}(\xi,\eta)Y_l^m(\eta,\phi) . \tag{7}$$

The changes with respect to the case of the spherically symmetric problem are now visible: Instead of separate equations for each angular momentum component l we have the matrix equations of the same form, coupling the various angular-momentum components. This parallelism with the spherical solutions will persist also for the whole response formalism below. We solved the set of coupled differential equations (5) numerically, i.e., without making use of any radial basis functions. Thereby, the expansion in multipolar components (3) was truncated at some chosen, state-dependent l value. With respect to this truncation, the choice of spheroidal coordinates turns out to be particularly rewarding, because they are "natural coordinates" for our problem. Usually just a few multipoles suffice to attain a very good numerical accuracy (e.g., ≈ 3 multipoles for the accuracy of $\approx 10^{-5}$ Ry per electron in the total energy for the ground-state calculation, in the size-range $3\le N\le 41$). For further results concerning the ground state the reader is referred to Ref. 12.

Within the TDLDA the central quantity to be obtained is the complex susceptibility $\chi(\mathbf{r},\mathbf{r}';\omega)$. Generally, within the TDLDA χ obeys the following integral equation:[8,9]

$$\chi(\mathbf{r},\mathbf{r}';\omega)=\chi_0(\mathbf{r},\mathbf{r}';\omega)+\int d^3\mathbf{r}_1\int d^3\mathbf{r}_2\chi_0(\mathbf{r},\mathbf{r}_2;\omega)K(\mathbf{r}_2,\mathbf{r}_1)\times\chi(\mathbf{r}_1,\mathbf{r}';\omega) . \tag{8}$$

In this equation the kernel $K(\mathbf{r}_2,\mathbf{r}_1)$ is given by[8,9]

$$K(\mathbf{r}_2,\mathbf{r}_1)=\frac{1}{|\mathbf{r}_2-\mathbf{r}_1|}+\delta(\mathbf{r}_1-\mathbf{r}_2)\left.\frac{dV_{\text{xc}}(n_-)}{dn_-}\right|_{n_-=n_-(\mathbf{r}_1)} , \tag{9}$$

where $n_-(\mathbf{r})$ is the ground-state electronic particle density distribution and dV_{xc}/dn_- is the density derivative of the local-density approximation (LDA) exchange-correlation potential[8,9] in the ground state. As explained in detail in Refs. 8 and 9 the independent particle susceptibility χ_0 is obtained from the occupied ground-state orbitals as follows:

$$\chi_0(\mathbf{r},\mathbf{r}';\omega)=\sum_{\substack{i\\ \text{occ}}}\psi_i^*(\mathbf{r})\psi_i(\mathbf{r}')G(\mathbf{r},\mathbf{r}';\varepsilon_i+\omega+i0^+)+\text{c.c.}(\omega\to-\omega) . \tag{10}$$

In this equation G is the retarded Green's function determined from the ground-state potential $V^{\text{eff}}(\mathbf{r})$ from the equation

$$[\tfrac{1}{2}\nabla^2-V^{\text{eff}}(\mathbf{r})+E]G(\mathbf{r},\mathbf{r}';E)=\delta(\mathbf{r}-\mathbf{r}') . \tag{11}$$

Due to the nonsphericity of $V^{\text{eff}}(\mathbf{r})$, G is *nondiagonal* with respect to the angular momentum L. Because of the assumed axial rotational (around the z axis) and reflectional (with respect to the midplane) symmetry of the problem, we can write

$$G(\mathbf{r},\mathbf{r}';E)\equiv G(\xi,\eta,\phi,\xi',\eta',\phi';E)=\sum_{M,P}\sum_{L,L'}Y_L^{*M}(\eta,\phi)G^{M,P}_{L,L'}(\xi,\xi';E)Y_{L'}^{M}(\eta',\phi') \tag{12}$$

where

$$P=+,-,\quad M=0,\pm1,\pm2,\ldots ,$$
$$L,L'=\begin{cases}|M|+2k, & P=+\\ |M|+2k+1, & P=-,\end{cases}\quad k=0,1,2,\ldots . \tag{13}$$

With the Dirac δ function in spheroidal coordinates[13]

$$\delta(\mathbf{r}-\mathbf{r}')=\frac{1}{a^2(\xi^2-\eta^2)}\delta(\xi-\xi')\delta(\eta-\eta')\delta(\phi-\phi') , \tag{14}$$

using expression (12) in Eq. (11) and performing an integration over angular coordinates as in obtaining Eq. (5), the matrix $G^{M,P}_{L,L'}(\xi,\xi';E)$ is determined as follows:

$$\sum_L \left[\frac{1}{2}\left[\frac{d}{d\xi}(\xi^2-1)\frac{d}{d\xi} - L(L+1) - \frac{M^2}{\xi^2-1} \right]\delta_{L',L} - V^M_{L',L}(a,\xi) + ED^M_{L',L}(a,\xi) \right] G^{M,P}_{L,L''}(\xi,\xi';E) = \delta(\xi-\xi')\delta_{L',L''} \ . \quad (15)$$

More details on obtaining the solutions for the Green's-function matrix $G^{M,P}_{L,L'}(\xi,\xi';E)$ are given in the Appendix. Having obtained $G^{M,P}_{L,L'}(\xi,\xi';E)$ and the ground-state solutions for the occupied levels (3) we can determine the independent-particle susceptibility χ_0. Once more, because the angular momentum is not conserved, we write

$$\chi_0(\mathbf{r},\mathbf{r}';\omega) = \sum_{M,P}\sum_{L,L'} Y^{*M}_L(\eta,\phi)[\chi_0]^{M,P}_{L,L'}(\xi,\xi';\omega) \times Y^M_{L'}(\eta',\phi') \ , \quad (16)$$

where, due to the restricted symmetry of the problem P,M,L,L' are allowed to take on values as in Eq. (13).

We can obtain the components $[\chi_0]^{M,P}_{L,L'}(\xi,\xi';\omega)$ straightforwardly from Eq. (10). If we use a similar expansion as in Eq. (16) for χ in the TDLDA response equation (8), we arrive at an equation for the various components of χ. In practice, we solve Eq. (8) on a grid in the ξ coordinate and truncate the angular-momentum expansion in Eq. (16). This leads to a set of coupled linear equations which can be solved straightforwardly. More details on constructing $[\chi_0]^{M,P}_{L,L'}(\xi,\xi';\omega)$ and calculating χ are given in the Appendix.

Anticipating the solution χ of Eq. (8) we turn to the solution of various polarizability tensor components: As explained in detail in Refs. 8 and 9 a general external potential $V^{\rm ext}(\mathbf{r};\omega)$ sets up an induced charge density $\rho^{\rm ind}(\mathbf{r};\omega)$, which is given by

$$\rho^{\rm ind}(\mathbf{r};\omega) = \int d^3\mathbf{r}'\,\chi(\mathbf{r},\mathbf{r}';\omega)V^{\rm ext}(\mathbf{r}';\omega) \ . \quad (17)$$

The induced charge density $\rho^{\rm ind}(\mathbf{r};\omega)$ gives rise to the induced *electrostatic* potential

$$V^{\rm ind}(\mathbf{r};\omega) = \int d^3\mathbf{r}'\frac{1}{|\mathbf{r}-\mathbf{r}'|}\rho^{\rm ind}(\mathbf{r}';\omega) \ . \quad (18)$$

For reasons which become clear immediately, we consider the response to a very special external field,

$$V^{\rm ext}(\mathbf{r};\omega) = -E^M_L(\omega)\frac{a^L}{C^{L-|M|}_{L,|M|}}P^{|M|}_L(\xi)Y^M_L(\eta,\phi) \ , \quad (19)$$

where the coefficient $C^{L-|M|}_{L,|M|}$ is the first coefficient in a series expansion of the associated Legendre polynomial $P^{|M|}_L(\xi)$ (Ref. 15) (see the Appendix).

Here the special form of $V^{\rm ext}$ has been taken, because we want to connect our formalism to the more conventional definition

$$V^{\rm ext}(\mathbf{r};\omega) \underset{a\xi\gg a}{\rightarrow} = -E^M_L(\omega)r^L Y^M_L(\cos\theta,\phi) \quad (a\xi\rightarrow r) \ . \quad (20)$$

That means for small eccentricity ($a \ll z_0$) (Refs. 12 and 13) or for distances far away from the spheroid, for which $a\xi\rightarrow r$,[13] where r is the radial distance from the center of the spheroid we recover the usually encountered perturbations (used for the definitions of multipolar polarizabilities[9]).

If the point $\mathbf{r}$ at which we observe the induced potential $V^{\rm ind}(\mathbf{r};\omega)$ is in the region outside the range of the induced electronic charge density of the cluster (where the induced charge density practically vanishes to zero for all computational purposes), then the quantities in expression (18) can be integrated out over the coordinate $\mathbf{r}'$ in a closed form and we obtain

$$V^{\rm ind}(\mathbf{r};\omega) = \sum_{L',M} Y^M_{L'}(\eta,\phi)\frac{(-1)^M}{a^{L'+1}\hat{C}^0_{L',|M|}}Q^{|M|}_{L'}(\xi) \times \alpha^M_{L',L}(\omega)E^M_L(\omega) \ , \quad (21)$$

where $\alpha^M_{L',L}(\omega)$ is the dynamical polarizability matrix. $Q^{|M|}_{L'}(\xi)$ and $\hat{C}^0_{L',|M|}$ in Eq. (21) are the associated Legendre function of the second kind and the first coefficient of its expansion in powers $1/\xi$ for $\xi>1$, respectively (see the Appendix).

The identification of $\alpha^M_{L',L}(\omega)$ as the polarizability matrix could be made, because we have for $a\xi \gg a$

$$\frac{(-1)^M}{a^{L'+1}\hat{C}^0_{L',|M|}}Q^{|M|}_{L'}(\xi) \underset{a\xi\gg a}{\rightarrow} \frac{1}{r^{L'+1}} \quad (r=a\xi) \ , \quad (22)$$

and for the case of a spherical ($a\rightarrow 0$), closed-shell cluster, all the equations and expressions of Ref. 9 are recovered. In this limit, the polarizability tensor $\alpha^M_{L',L}(\omega)$ becomes the usually encountered L-pole dynamical polarizability $\alpha_L(\omega)$ (Ref. 9)

$$\alpha^M_{L',L}(\omega) \underset{a\rightarrow 0}{\rightarrow} \alpha_L(\omega)\delta_{L',L} \ . \quad (23)$$

This can be a useful check of the numerics: Calculate the spherical result via spheroidal code. More details on the derivation of Eqs. (17)–(23) are given in the Appendix.

The important and new feature for open-shell clusters—in contrast to the closed-shell ones (for $N=2,8,20,40,58,91$)—is that the angular momentum of the external field $E^M_L(\omega)$ is *not conserved*. The charge density and potential, induced by $E^M_L(\omega)$ consist of *many* multipolar components.

Surprisingly enough, this feature has been overlooked in all recent work about this subject. Tacitly, this was the reason why in Refs. 8 and 9, by one of us (W.E.), only the closed-shell clusters were explicitly studied. Another interesting feature is the M dependence of the polarizability $\alpha^M_{L',L}(\omega)$ which in effect leads to different polarizabilities along different axes of the spheroid.

III. RESULTS AND DISCUSSION

The simplest case to study is the response to a homogeneous external field along the z axis, the axis of the rotational symmetry of the spheroid, where the electrostatic potential is

$$V_z^{\text{ext}}(\mathbf{r};\omega) = -E_z(\omega) z \ ,$$

or, in (prolate) spheroidal coordinates

$$V_z^{\text{ext}}(\mathbf{r};\omega) = -E_1^0(\omega)\frac{a}{C_{1,0}^1} P_1^0(\xi) Y_1^0(\eta,\phi)$$

$$\text{with } E_1^0(\omega) \equiv \left[\frac{4\pi}{3}\right]^{1/2} E_z(\omega) \ , \quad (24)$$

and to the homogeneous field, perpendicular to the z axis, with the electrostatic potential

$$V_\rho^{\text{ext}}(\mathbf{r};\omega) = -E_\rho(\omega)\rho \ ,$$

or, in (prolate) spheroidal coordinates

$$V_\rho^{\text{ext}}(\mathbf{r};\omega) = E_1^1(\omega)\frac{a}{C_{1,1}^0} P_1^1(\xi)\tfrac{1}{2}[Y_1^1(\eta,\phi) - Y_1^{-1}(\eta,\phi)]$$

$$\text{with } E_1^1(\omega) = \left[\frac{8\pi}{3}\right]^{1/2} E_\rho(\omega) \ . \quad (25)$$

With the help of these external fields the polarizability-matrix components $\alpha_{L',1}^0(\omega)$ and $\alpha_{L',1}^\mu(\omega)$ $(\mu = +1, -1)$ can be calculated, where for obvious reasons we write

$$\alpha_z(\omega) \equiv \alpha_{1,1}^0(\omega) \quad (26)$$

and

$$\alpha_\rho(\omega) \equiv \tfrac{1}{2}[\alpha_{1,1}^1(\omega) - \alpha_{1,1}^{-1}(\omega)] \ . \quad (27)$$

Because of the restricted computer time, we give in what follows just the result for one particle number, namely $N = 10$. We chose this particle number because, for $N = 10$, the ground-state calculations give us a pronounced prolate spheroid with the major-to-minor axis ratio $z_0/\rho_0 = 1.63$, and furthermore, the experimental polarizability[16,17] and photoabsorption cross-section results[17] exist for this particle size.

The static results for $N = 10$ are

$$\alpha_z(0)/R^3 = 2.15, \quad \alpha_\rho(0)/R^3 = 1.20 \ ,$$

and defining an average polarizability,

$$\alpha_{\text{av}}(0) = \tfrac{1}{3}[\alpha_z(0) + 2\alpha_\rho(0)] = 1.52R^3 \ .$$

This is to be compared with the experimental value[16]

$$\alpha_{\text{av}}^{\text{expt}}(0) = 2.02R^3 \ .$$

As it was for the spherical case (the closed-shell cluster case) the theoretical polarizability is too low by about 20% with respect to the experimental values.[2,16] For reasons discussed recently by Stampfli and Bennemann,[18] the main reason for this deficiency of the TDLDA lies in the following: Within the TDLDA each electron is subject to the action of the external field plus the mean field, produced by the polarization of all the electrons, including itself. This means that even a single electron under the influence of an external field will feel an additional field due to its own contribution to the induced charge. This "self-interaction" is, of course, unphysical and is an intrinsic flaw of the formalism, which should in principle be corrected.

Too low static polarizability in the TDLDA will be in turn related to too high frequencies for the dynamical electronic excitations, of about 10–15 %, since dynamical and static properties of the excitation spectrum are connected by the sum rules.[19] Aside from these changes, all other spectral features (spectral structure and oscillator strengths) are expected to be the same. Of course, the intrinsic flaws of the TDLDA have to be corrected also for the dynamical case, as it was done for the static one.[18] However, even for a static case the self-interaction correction requires a great deal of numerical effort. This would be even much more difficult for the dynamical case. So, until this is done, the TDLDA remains the best theory for investigating the dynamical electronic response properties of systems, based on the ground-state local-density approximation calculation.

As was the case for spherical clusters, we expect the spectrum [for *each* polarizability $\alpha_z(\omega)$ and $\alpha_\rho(\omega)$] to consist of single-pair lines and a surface-plasmon line, where generally the lines are at different positions for α_z and α_ρ. Because the photoabsorption cross section $\sigma(\omega)$ is proportional to $\text{Im}\alpha(\omega)$,[8,9] the imaginary part of the dynamical polarizability is in the focus of interest. In comparison to the spherical case, discussed in detail in Refs. 8 and 9, the polarizability is directionally dependent, with (of course) different screening properties along the symmetry axis and perpendicular to it. Hence we present in Figs. 1(a) and 1(b) the various components of $\alpha(\omega)$ and in Fig. 1(c) the "equivalent" spherical $\alpha(\omega)$ for $N = 10$. Similar to Refs. 8 and 9, the small numerical damping, $\Delta = 10^{-3}$ Ry $= 0.0136$ eV was used, instead of the positive infinitesimal 0^+ in Eq. (10). This was done for purely numerical reasons, in order to avoid divergencies around the poles of the Green's function, defined in Eq. (11). Such a small value of Δ does not affect the calculated spectral structure and spectral weights.

In all figures the dotted line gives the result for α using a χ_0, which means "screening without electron-electron interaction," or more physically "screening without collective effects;" and the solid line gives the full TDLDA $\alpha(\omega)$. We want to stress once more that Fig. 1(c) is intrinsically wrong, because it ignores the coupling of various angular momenta discussed above. Both $\alpha_z(\omega)$ and $\alpha_\rho(\omega)$ show a considerable amount of fragmentation of the total oscillator strength, as was the case for $N = 20$ in the spherical case (discussed in detail in Ref. 8). It seems presently impossible to assign one line as being a collective one. This seems to indicate the microscopic breakdown of any plasmon-pole approximation. If we ignore this for a moment, the application of the surface-plasmon-pole approximation[20,8] would give us the vertical lines in Figs. 1(a)–1(c) for the corresponding surface-plasmon frequencies, in agreement with[20,8]

$$\omega^{\text{plasmon}} = \left[\frac{\alpha^{\text{cl}}(0)}{\alpha(0)}\right]^{1/2} \omega^{\text{cl}} \ , \quad (28)$$

with the classical static polarizability $\alpha^{\text{cl}}(0)$ given by

$$\alpha^{\text{cl}}(0) = R^3 \quad (29)$$

and the classical Mie frequency given by

$$\omega_{\rm cl}=\frac{1}{r_S^{3/2}}\ \text{a.u.}\ , \tag{30}$$

where the Wigner-Seitz radius is

$$r_S/a_0=4$$

for Na, with a_0 the Bohr radius.

None of the figures discussed so far can be directly compared to the experimental data, where one measures the directional average of the photoabsorption cross section $\sigma(\omega)$. Therefore we present in Fig. 2(a) this directionally averaged quantity

$$\sigma(\omega)=\frac{4\pi\omega}{3c}[\mathrm{Im}\alpha_z(\omega)+2\,\mathrm{Im}\alpha_\rho(\omega)]\ , \tag{31}$$

which looks rather different from Fig. 1(c). Hence we see that it really does not make sense to describe open-shell clusters by the spherical picture, as is very often done in the literature (e.g., Ref. 21).

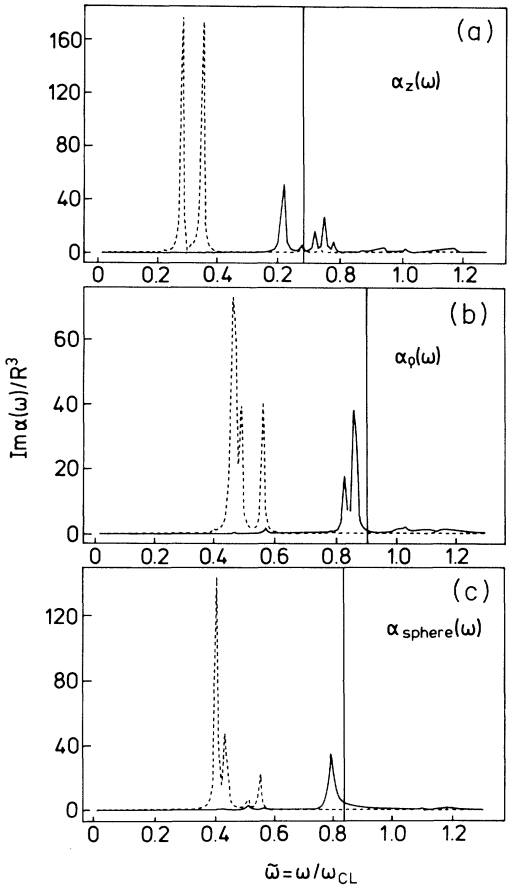

FIG. 1. Imaginary part of the various complex-dipole polarizabilities for the Na_{10} cluster, in units of R^3, with $R=N^{1/3}r_S$, with $N=10$ and $r_S=4$ Bohr for Na. (a) Shows the z component $\alpha_z(\omega)$ and (b) shows the ρ component for polarization perpendicular to the symmetry axis. The frequency is in units of the classical Mie frequency for Na, $\omega_{\rm cl}=0.250$ Ry [Eq. (30)]. Solid line, TDLDA; dashed line, independent-particle response, sometimes called LDA polarizability. (c) gives Im$\alpha(\omega)$ in the spherical approximation, which is—for open-shell clusters—clearly insufficient. In all figures the vertical line gives the position of the dipolar surface-plasma frequency obtained from the sum-rule equation (28) of the main text, using the corresponding, microscopically calculated static polarizability for each case. This sum-rule description fails to reproduce the microscopic fragmentation of the plasmon line observed for both polarizabilities [see (a) and (b)]. This fragmentation is a particle-hole pair effect in the same way as discussed for the spherical case for $N=20$ in Ref. 9. The collective nature of excitations can be identified as described in detail in Ref. 9.

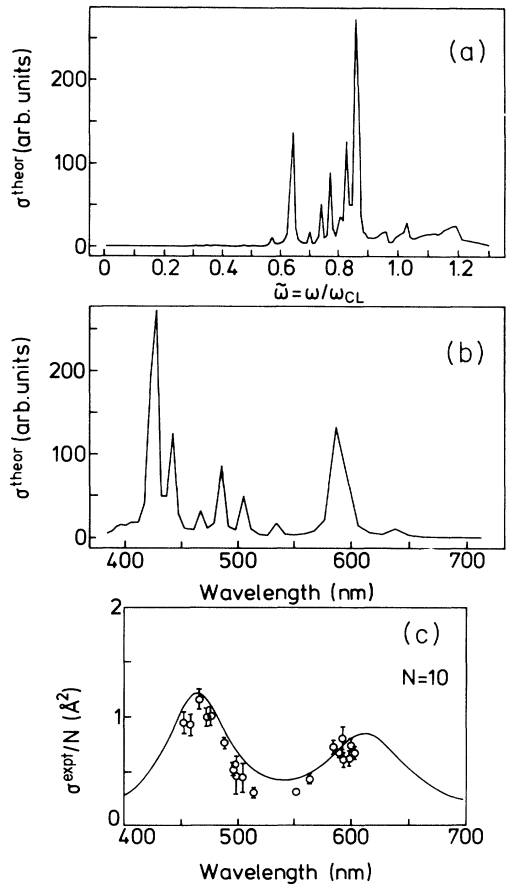

FIG. 2. (a) Orientational average of the photoabsorption cross section of the Na_{10} cluster, following from Eq. (31) of the main text, as a function of frequency $\tilde\omega=\omega/\omega_{\rm cl}$, with $\omega_{\rm cl}$ the classical Mie frequency [Eq. (30)]. (b) Same as (a) as a function of *wavelength*, shown in the energy window $0.59\le\tilde\omega\le0.95$, which is similar to that of the experimental spectrum (c). (c) Photoabsorption cross section of the Na_{10} cluster, as measured by the Berkeley group (Ref. 17). The solid line is a so-called theory curve of Ref. 17, obtained from the surface-plasmon-pole approximation with an arbitrary damping $\Gamma=0.15\omega_{\rm plasma}$. For more details see Ref. 17. On comparing theory (b) with experiment (c) we see that the plasmon line *positions* are in fair agreement (within the limits of accuracy of the TDLDA, as discussed in the text). However, the theoretically determined linewidth is seriously in error. The reason is that at the present level of theory the coupling of the plasmon line to thermal cluster-shape fluctuations is missing (Ref. 10). A calculation along this line has been completed (Ref. 11).

To facilitate comparison with experiment we present in Fig. 2(b) the cross section as a function of wavelength (in nm) in the range where experimental data are available.[17] On looking at these figures, we think it is premature to conclude that the plasmon-pole approximation is the right way to interpret the experimental data. In contrast, as was discussed in detail in Ref. 9 for $N=20$, at those low particle numbers everything is coupled together and only the microscopic response formalism is able to account for all the complexity of $\sigma(\omega)$.

If one *artificially* broadens the sum-rule vertical line with a lifetime, the broadened line overlaps with the microscopically calculated lines [the solid line in Fig. 2(c)]. But this is not a valid procedure. This agreement is in our view a brute-force fitting result. In order to accentuate this we stress that no first-principle microscopic theory can produce such a big damping of collective excitations, as the one resulting from this fitting procedure ($\approx 15\%$ of the surface plasmon frequency). The full possibility of Landau damping within the TDLDA is given in our calculation, which takes into account all one-electron excitation channels. The probability for the higher-order (two-electron two-hole) excitations, going beyond the TDLDA, is negligible for so small particles, as considered here.[22]

In our view, the most reasonable explanation for the origin of so broad experimental photoabsorption features is therefore the one recently proposed by Pacheco and Broglia:[10] The clusters in molecular-beam experiments are not frozen, but they isomerize. The most important vibrational mode influencing the dipole photoabsorption cross-section frequencies are the quadrupolar ellipsoidal shape fluctuations.[10] For every different shape of the cluster the sharp absorption lines of Fig. 2(b) will lie in slightly different positions. As the shape fluctuation frequencies are approximately three orders of magnitude larger than the frequencies of photoabsorption-induced electronic transitions, one records in the photoabsorption experiment the superposition of all the photoabsorption spectra as in Fig. 2(b), corresponding to the average over all the thermally excited cluster shapes. So, the overlap of a multitude of sharp spectral lines as in Fig. 2(b) yields the broad experimental photoabsorption structure of Fig. 2(c). We recently completed work along these lines in the framework of our model, obtaining very good agreement with experiment.[11]

IV. CONCLUSION

A fairly complete description of the dynamical polarizability of small open-shell clusters is given within the frame of the time-dependent local-density approximation (TDLDA) applied to the self-consistent spheroidal jellium model. Also, it was discussed why the very popular semiclassical approach[19] to the spectra can be misleading in interpreting the experimental data, in view of the detailed description given in this paper. Certainly, the sum-rule description results in an *artificially broad damping* to account for the line fragmentation found microscopically [see especially Fig. 2(b)]. Also, it might well be that the sum-rule description results in the *wrong* frequencies for the plasmons. Missing in the present formalism are the ionic structure effects. However, similar to plasmons in real solids of Na, K, and Li,[23] excepting damping, those effects are expected to play a minor role. We expect the ionic cores to introduce the additional plasmon fragmentation channels, which will correspond to an additional damping in the bulk solids.[24]

A definite answer concerning the problem of linewidths of photoabsorption spectral structures can be given, introducing in the present formalism the coupling to shape fluctuations as proposed by Pacheco and Broglia,[10] and this was presented in Ref. 11. Furthermore, we would like to mention that the breakdown of the sum-rule interpretation for $N=20$ (Ref. 8) has also been pointed out by Yannouleas *et al.*[25]

ACKNOWLEDGMENTS

The authors are grateful to Professor Dr. Elmar Zeitler for continuing interest and support. One of us (Z.P.) is financially supported by the Deutsche Forschungsgemeinschaft through the SPP "Physik anorganischer Cluster."

APPENDIX

In this appendix we shall give more details on the calculation of the Green's function (12) and on the derivation of the dynamical polarizability tensors $\alpha^{M}_{L',L}(\omega)$ in Eq. (21). Let us write once again the matrix differential equation for the Green's-function matrix $G^{M,P}_{L,L''}(\xi,\xi';E)$ [Eq. (15)]:

$$\sum_{L}\left[\frac{1}{2}\left[\frac{d}{d\xi}(\xi^2-1)\frac{d}{d\xi}-L(L+1)-\frac{M^2}{\xi^2-1}\right]\delta_{L',L}-V^{M}_{L',L}(a,\xi)+ED^{M}_{L',L}(a,\xi)\right]G^{M,P}_{L,L''}(\xi,\xi';E)=\delta(\xi-\xi')\delta_{L',L''}\ . \quad \text{(A1)}$$

From the textbook solutions[26,27] we know how the Green's-function matrix $G^{M,P}_{L,L'}(\xi,\xi';E)$ can be constructed from appropriate solutions of the Schrödinger-like equation (5). Explicitly, we have[26,27]

$$G^{M,P}_{L,L'}(\xi,\xi';E)=-2\sum_{L'',L'''}\begin{cases} j^{M,P}_{L,L''}(\xi;E)[W^{M,P}(E)]^{-1}_{L'',L'''}[h^{\tilde{M},P}(\xi';E)]_{L''',L'}, & \xi<\xi' \\ h^{M,P}_{L,L''}(\xi;E)[W^{\tilde{M},P}(E)]^{-1}_{L'',L'''}[j^{\tilde{M},P}(\xi';E)]_{L''',L'}, & \xi\geq\xi' \end{cases} \quad \text{(A2)}$$

Let us assume that in the expansion of the wave function, Eq. (3), generally $\lambda_{\max}$ different l values appear. In this case, the matrices $j^{M,P}_{L,L''}(\xi;E)$ and $h^{M,P}_{L,L''}(\xi;E)$ in Eq. (A2) have a dimension $\lambda_{\max}$ by $\lambda_{\max}$. Then, the $\lambda_{\max}$ columns of $j^{M,P}_{L,L''}(\xi;E)$ are given by the "radial" parts of the various linearly independent solutions of Eq. (5) with $\varepsilon_i \to E$, regular at

the origin of the radial coordinate ξ. The matrix $h^{M,P}_{L,L''}(\xi;E)$ is defined in exactly the same way, but the various solutions now fulfill outgoing wave boundary conditions.[8,9]

Finally, the Wronskian matrix $W^{M,P}_{L,L'}(E)$ is defined as follows:

$$W^{M,P}_{L,L'}(E)=(\xi^2-1)\sum_{L''}\left\{[h^{\tilde{M},P}(\xi;E)]_{L,L''}\left[\frac{d}{d\xi}j^{M,P}_{L'',L'}(\xi;E)\right]-\left[\left[\frac{d}{d\xi}h^{\tilde{M},P}(\xi;E)\right]_{L,L''}\right]j^{M,P}_{L'',L'}(\xi;E)\right\} . \tag{A3}$$

The derivative operator $d/d\xi$ in the second set of large parentheses on the right-hand side (rhs) of Eq. (A3) is active just inside these parentheses. The Wronskian matrix is independent of ξ. In Eqs. (A2) and (A3) the tilde denotes the transpose of a given matrix.

Having obtained the Green's-function matrix $G^{M,P}_{L,L'}(\xi,\xi';E)$ and the ground-state solutions for the occupied levels, we can determine the independent-particle susceptibility χ_0 [Eq. (16)]

$$\chi_0(\mathbf{r},\mathbf{r}';\omega)=\sum_{M,P}\sum_{L,L'}Y^{*M}_L(\eta,\phi)[\chi_0]^{M,P}_{L,L'}(\xi,\xi';\omega)Y^M_{L'}(\eta',\phi') . \tag{A4}$$

From Eqs. (10), (12), and (3) it straightforwardly follows that the angular-momentum matrix components $[\chi_0]^{M,P}_{L,L'}(\xi,\xi';\omega)$ are constructed as

$$[\chi_0]^{M,P}_{L,L'}(\xi,\xi';\omega)=\sum_{m,p,n}\nu_{m,p,n}\sum_{l,l'}\sum_{L'',L'''}\left\langle\begin{matrix}L & l & L''\\ M & m & M-m\end{matrix}\right\rangle\left\langle\begin{matrix}L' & l' & L'''\\ M & m & M-m\end{matrix}\right\rangle$$
$$\times[X^{m,p}_l(\xi;\varepsilon_{m,p,n})G^{M-m,(Pp)}_{L'',L'''}(\xi,\xi';\varepsilon_{m,p,n}+\omega+i\Delta)X^{m,p}_{l'}(\xi',\varepsilon_{m,p,n})+\text{c.c.}(\omega\to-\omega)] , \tag{A5}$$

where $\nu_{m,p,n}$ are occupation numbers of Kohn-Sham orbitals $\psi_{m,p,n}$ in the ground state. In (A5) we introduced the notation

$$\left\langle\begin{matrix}L & l & l'\\ M & m & m'\end{matrix}\right\rangle=\int_0^{2\pi}d\phi\int_{-1}^{1}d\eta\,Y^M_L(\eta,\phi)Y^{*m}_l(\eta,\phi)\times Y^{*m'}_{l'}(\eta,\phi) . \tag{A6}$$

In a similar way, we may now construct explicit equations for the multipolar matrix components of the self-consistently screened TDLDA susceptibility (8),

$$\chi(\mathbf{r},\mathbf{r}';\omega)=\sum_{M,P}\sum_{L,L'}Y^{*M}_L(\eta,\phi)[\chi]^{M,P}_{L,L'}(\xi,\xi',\omega)Y^M_{L'}(\eta',\phi') . \tag{A7}$$

The Coulomb interaction $1/|\mathbf{r}_1-\mathbf{r}_2|$, appearing in the kernel (9), can be written in spheroidal coordinates as[28]

$$\frac{1}{|\mathbf{r}_1-\mathbf{r}_2|}=\sum_{L=0}^{\infty}\sum_{M=-L}^{L}Y^{*M}_L(\eta,\phi)U^M_L(\xi,\xi')Y^M_L(\eta',\phi') \tag{A8}$$

with

$$U^M_L(\xi,\xi')=(-1)^M\frac{4\pi}{a}\frac{(L-|M|)!}{(L+|M|)!}[P^{|M|}_L(\xi_<)Q^{|M|}_L(\xi_>)] , \tag{A9}$$

where

$$\xi_<=\min(\xi,\xi'),\quad \xi_>=\max(\xi,\xi') ,$$

and where $P^{|M|}_L(\xi)$ and $Q^{|M|}_L(\xi)$ are associated Legendre functions of the first and second kind, respectively.[15]

Also, we can in principle introduce the multipolar expansion of the second term on the rhs of Eq. (9),

$$\left.\frac{\partial V_{\text{xc}}[n_-]}{\partial n_-}\right|_{n_-=n_-(\mathbf{r})}=\sum_{l=0}^{\infty}Y^0_{2l}(\eta,\phi)[V'_{\text{xc}}]_{2l}(\xi) . \tag{A10}$$

We introduce the matrix $B^M_{L,L'}(\xi)$, whose matrix elements are

$$B^M_{L,L'}(\xi)=\sum_l\left\langle\begin{matrix}L' & L & 2l\\ M & M & 0\end{matrix}\right\rangle[V'_{\text{xc}}]_{2l}(\xi) , \tag{A11}$$

with $[V'_{\text{xc}}]_{2l}(\xi)$ given in Eq. (A10). As the derivative of the local-density exchange-correlation potential on the left-hand side (lhs) of Eq. (A10) contains unphysical cusps whose angular-momentum expansion converges very slowly, we retained only the $l=0$ (spheroidally averaged) term on the rhs of Eq. (A10) in the first practical calculations performed. Integration over angular coordinates in Eq. (8) gives us a matrix integral equation, coupling multipolar components, similarly as in Eqs. (5) and (15):

$$[\chi]^{M,P}_{L,L'}(\xi,\xi';\omega)=\sum_{L_1,L_2,L_3}a\int_1^{\infty}d\xi_1\left\{\frac{1}{a}\delta_{L,L_3}\delta(\xi-\xi_1)-[\chi_0]^{M,P}_{L,L_1}(\xi;\xi_1;\omega)B^M_{L_1,L_2}(\xi_1)D^M_{L_2,L_3}(\xi_1)\right.$$
$$\left.-a\int_1^{\infty}d\xi_2[\chi_0]^{M,P}_{L,L_1}(\xi;\xi_2;\omega)D^M_{L_1,L_2}(\xi_2)U^M_{L_2}(\xi_2,\xi_1)D^M_{L_2,L_3}(\xi_1)\right\}[\chi]^{M,P}_{L_3,L'}(\xi_1,\xi';\omega) . \tag{A12}$$

In practice, we solved Eq. (A12) as a set of linear equations, using the discrete number of mesh points ξ and truncating the multipolar matrix expansions, as already discussed. We may now do the final step, deriving the expressions for the dynamical polarizability tensor $\alpha^{M}_{L',L}(\omega)$.

As explained in detail in Refs. 8 and 9 a general external potential $V^{\text{ext}}(\mathbf{r};\omega)$ sets up an induced charge density $\rho^{\text{ind}}(\mathbf{r};\omega)$, which is given by

$$\rho^{\text{ind}}(\mathbf{r};\omega)=\int d^3r'\chi(\mathbf{r},\mathbf{r}';\omega)V^{\text{ext}}(\mathbf{r}';\omega)\ . \tag{A13}$$

This induced charge density gives rise to the induced electrostatic potential

$$V^{\text{ind}}(\mathbf{r};\omega)=\int d^3r'\frac{1}{|\mathbf{r}-\mathbf{r}'|}\rho^{\text{ind}}(\mathbf{r}';\omega)\ . \tag{A14}$$

All of these quantities can be expanded in spherical harmonics,

$$\begin{aligned} V^{i}(\mathbf{r};\omega)&=\sum_{L,M}[V^{i}]^{M}_{L}(\xi;\omega)Y^{M}_{L}(\eta,\phi),\quad i=(\text{ext},\text{ind})\ ,\\ \rho^{\text{ind}}(\mathbf{r};\omega)&=\sum_{L,M}[\rho^{\text{ind}}]^{M}_{L}(\xi;\omega)Y^{M}_{L}(\eta,\phi)\ . \end{aligned} \tag{A15}$$

So, Eqs. (A13) and (A14) give, after integration over angular coordinates with the help of Eqs. (A15), (A8), (A9), and (6),

$$[\rho^{\text{ind}}]^{M}_{L}(\xi;\omega)=\sum_{L',L''}a\int_{1}^{\infty}d\xi'\chi^{M,P}_{L,L'}(\xi,\xi';\omega)\times D^{M}_{L',L''}(\xi)[V^{\text{ext}}]^{M}_{L''}(\xi';\omega)\ , \tag{A16}$$

$$[V^{\text{ind}}]^{M}_{L}(\xi;\omega)=\sum_{L'}a\int_{1}^{\infty}d\xi' U^{M}_{L}(\xi,\xi')D^{M}_{L,L'}(\xi')\times[\rho^{\text{ind}}]^{M}_{L'}(\xi';\omega)\ . \tag{A17}$$

Because of the open-shell structure, the response of the system is nondiagonal with respect to the angular momentum. However, due to the chosen restricted symmetry, the parity P and the azimuthal quantum number M are being conserved.

We consider the response to a very special external field,

$$V^{\text{ext}}(\mathbf{r};\omega)=-E^{M}_{L}(\omega)\frac{a^{L}}{C^{L-|M|}_{L,|M|}}P^{|M|}_{L}(\xi)Y^{M}_{L}(\eta,\phi)\ , \tag{A18}$$

where the coefficients $C^{L-|M|}_{L,|M|}$ are the coefficients in a series expansion of the associated Legendre polynomial $P^{|M|}_{L}(\xi)$ of the first kind,[15]

$$\begin{aligned} P^{|M|}_{L}(\xi)&=(\xi^2-1)^{|M|/2}\frac{d^{|M|}}{d\xi^{|M|}}P_{L}(\xi)\\ &=\sum_{j=[(L+|M|)/2]}^{L}(\xi^2-1)^{|M|/2}C^{2j-L-|M|}_{L,|M|}\xi^{2j-L-|M|}\\ &\qquad\text{where } [x]\equiv\text{smallest integer}\geq x\ . \end{aligned} \tag{A19}$$

The form and the normalization of the external potential is taken, as given in Eq. (A13), because besides satisfying the Laplace equation

$$\nabla^2V^{\text{ext}}(\mathbf{r};\omega)=0\ , \tag{A20}$$

in the limit $a\xi\gg a$ (for small eccentricities or large distances from the spheroid, when $a\xi\rightarrow r$) the external electrostatic field (A18) becomes a (L,M) multipolar external field in spherical coordinates

$$V^{\text{ext}}(\mathbf{r};\omega)=-E^{M}_{L}(\omega)r^{L}Y^{M}_{L}(\cos\theta,\phi)\ , \tag{A21}$$

which is usually used as an external field in studying the multipolar electronic response.[9] r,θ,ϕ is the standard notation for the radial and the two angular coordinates of the polar spherical coordinate system, respectively.

If the point $\mathbf{r}$ at which we observe the induced potential $V^{\text{ind}}(\mathbf{r};\omega)$ is in the region outside the range of the induced electronic charge density of the cluster (where the induced charge density practically vanishes to zero for all computational purposes), then $\xi>\xi'$ in Eq. (A17), and using Eqs. (A8) and (A9) we have

$$V^{\text{ind}}(\mathbf{r};\omega)=\sum_{L',M}(-1)^{M}\frac{4\pi}{a}\frac{(L'-|M|)!}{(L'+|M|)!}Q^{|M|}_{L'}(\xi)Y^{M}_{L'}(\eta,\phi)\sum_{L''}a\int_{1}^{\infty}d\xi' P^{|M|}_{L''}(\xi')D^{M}_{L',L''}(\xi')[\rho^{\text{ind}}]^{M}_{L''}(\xi';\omega)\ , \tag{A22}$$

where for the special external potential, Eq. (A18), and using Eq. (A16) the induced charge density is given by

$$[\rho^{\text{ind}}]^{M}_{L''}(\xi';\omega)=\sum_{L'''}a\int_{1}^{\infty}d\xi''\chi^{M,P}_{L'',L'''}(\xi',\xi'';\omega)D^{M}_{L''',L}(\xi'')\frac{a^{L}}{C^{L-|M|}_{L,|M|}}P^{|M|}_{L}(\xi'')[-E^{M}_{L}(\omega)]\ . \tag{A23}$$

Since by using expressions in Ref. 15, we can expand $Q^{|M|}_{L'}(\xi)$ (for $|\xi|>1$)

$$Q^{|M|}_{L'}(\xi)=(-1)^{M}(\xi^2-1)^{|M|/2}\sum_{n=0}^{\infty}\hat{C}^{2n}_{L',|M|}\frac{1}{\xi^{L'+|M|+2n+1}}\ . \tag{A24}$$

It is reasonable to rewrite Eq. (A22) as follows:

$$V^{\text{ind}}(\mathbf{r};\omega)=\sum_{L',M}Y^{M}_{L'}(\eta,\phi)\frac{(-1)^{M}}{a^{L'+1}\hat{C}^{0}_{L',|M|}}Q^{|M|}_{L'}(\xi)\alpha^{M}_{L',L}(\omega)E^{M}_{L}(\omega)\ , \tag{A25}$$

where we have defined the polarizability matrix $\alpha^{M}_{L',L}(\omega)$ as follows:

$$\alpha^{M}_{L',L}(\omega)=(2L+1)\frac{(L'-|M|)!}{(L'+|M|)!}\hat{C}^{0}_{L',|M|}a\int_{1}^{\infty}d\xi' a^{L'}P^{|M|}_{L'}(\xi')\alpha^{M}_{L',L}(\xi';\omega)\ . \tag{A26}$$

Here, the matrix of the polarization charge density is given as

$$\alpha^{M}_{L',L}(\xi';\omega)=-\frac{4\pi}{2L+1}\sum_{L''}D^{M}_{L',L''}(\xi')\sum_{L'''}a\int_{1}^{\infty}d\xi''\chi^{M,P}_{L'',L'''}(\xi',\xi'';\omega)D^{M}_{L''',L}(\xi'')\frac{a^{L}}{C^{L-|M|}_{L,|M|}}P^{|M|}_{L}(\xi'')\ . \tag{A27}$$

The identification of $\alpha^{M}_{L',L}(\omega)$ in Eq. (A26) could be made, because for $a\xi\gg a$

$$\frac{(-1)^{M}}{a^{L'+1}\hat{C}^{0}_{L',|M|}}Q^{|M|}_{L'}(\xi)\underset{a\xi\gg a}{\rightarrow}\frac{1}{r^{L'+1}}\quad(r=a\xi)\ , \tag{A28}$$

and additionally, for the case of a spherical ($a\rightarrow 0$), closed-shell cluster, all the quantities in our spheroidal response equations go over to the corresponding quantities for the spherically symmetric problem of Ref. 9. In this limit, $[V^{\rm eff}]^{m}_{l',l}(a,\xi)\rightarrow[V^{\rm eff}]^{0}_{0,0}(r)\delta_{l,0}\delta_{l',0}$ in Eq. (6), because of spherical symmetry. From this it follows that Eq. (5) becomes decoupled for various l values. [The wave-function expansion (3) contains just *one* angular-momentum component.] All of the m states belonging to a given l value, $m=-l,-(l-1),\ldots,(l-1),l$, are degenerate and all $\nu_{m,p,n}$ are equal within this group. Also, due to the same reasons $G^{M,P}_{L,L''}(\xi,\xi';E)\rightarrow G_{L}(r,r';E)\delta_{L,L''}$. It is then straightforward to show, by using the properties of the integrals of three spherical harmonics (A6),[29] that in this limit the expression (A5) goes over to

$$[\chi_0]^{M,P}_{L,L'}(\xi,\xi';\omega)\underset{a\rightarrow 0}{\rightarrow}[\chi_0]_{L}(r,r';\omega)\delta_{L,L'}\ , \tag{A29}$$

where $[\chi_0]_L(r,r';\omega)$ is the L-pole independent-particle susceptibility for the spherically symmetric problem.[9] In this case it directly follows

$$\chi^{M,P}_{L,L'}(\xi,\xi';\omega)\underset{a\rightarrow 0}{\rightarrow}\chi_{L}(r,r';\omega)\delta_{L,L'}\ , \tag{A30}$$

and according to this

$$\alpha^{M}_{L,L'}(\xi;\omega)\underset{a\rightarrow 0}{\rightarrow}\alpha_{L}(r;\omega)\delta_{L,L'}\ , \tag{A31}$$

where $\chi_L(r,r';\omega)$ and $\alpha_L(r;\omega)$ are the L-pole TDLDA susceptibility and the polarizability density of the rotationally invariant electronic system, respectively,[9] fulfilling the relations

$$\alpha_{L}(r,\omega)=-\frac{4\pi}{2L+1}r^{2}\int_{0}^{\infty}dr'(r')^{L+2}\chi_{L}(r,r';\omega) \tag{A32}$$

and

$$\alpha_{L}(\omega)=\int_{0}^{\infty}dr\,r^{L}\alpha_{L}(r;\omega)\ . \tag{A33}$$

*On leave of absence from the Institute of Physics of the University of Zagreb, Croatia, Yugoslavia.

[1]W. Ekardt, Phys. Rev. B **29**, 1558 (1984).

[2]W. Ekardt, Phys. Rev. Lett. **52**, 1925 (1984).

[3]M. Y. Chou, A. Cleland, and M. L. Cohen, Solid State Commun. **52**, 645 (1984).

[4]D. E. Beck, Solid State Commun. **49**, 381 (1984).

[5]D. E. Beck, Phys. Rev. B **35**, 7325 (1987).

[6]M. J. Puska, R. M. Nieminen, and M. Manninen, Phys. Rev. B **31**, 3486 (1985).

[7]W. Ekardt and Z. Penzar, Phys. Rev. B **38**, 4273 (1988).

[8]W. Ekardt, Phys. Rev. B **31**, 6360 (1985).

[9]W. Ekardt, Phys. Rev. B **32**, 1961 (1985).

[10]J. M. Pacheco and R. A. Broglia, Phys. Rev. Lett. **62**, 1400 (1989).

[11]Z. Penzar, W. Ekardt, and A. Rubio, Phys. Rev. B **42**, 5040 (1990).

[12]Z. Penzar and W. Ekardt (unpublished).

[13]P. M. Morse and H. Feshbach, *Methods of Theoretical Physics* (McGraw-Hill, New York, 1953).

[14]In this work we explicitly write only the equations for the prolate spheroidal coordinates. All the expressions for the oblate case are obtained by simultaneously replacing $\xi\rightarrow\pm i\xi$, $a\rightarrow\mp ia$.

[15]*Handbook of Mathematical Functions,* edited by M. Abramowitz and I. A. Stegun (Dover, New York, 1964).

[16]W. D. Knight, K. Clemenger, W. A. de Heer, and W. A. Saunders, Phys. Rev. B **31**, 2539 (1985).

[17](a) W. A. de Heer, K. Selby, V. Kresin, J. Masui, M. Vollmer, A. Châtelain, and W. D. Knight, Phys. Rev. Lett. **59**, 1805 (1987); (b) K. Selby, M. Vollmer, J. Masui, V. Kresin, W. A. de Heer, and W. D. Knight, Phys. Rev. B **40**, 5417 (1989).

[18](a) P. Stampfli and K. H. Bennemann, Phys. Rev. A **39**, 1007 (1989); (b) P. Stampfli and K. H. Bennemann, in *Physics and Chemistry of Small Clusters, NATO Advanced Study Institute, Series B: Physics,* edited by P. Jena, B. K. Rao, and S. N. Khanna (Plenum, New York, 1987).

[19]G. Bertsch and W. Ekardt, Phys. Rev. B **32**, 7659 (1985).

[20]W. Ekardt, D. B. Tran Thoai, F. Frank, and W. Schulze, Solid State Commun. **46**, 571 (1983).

[21]M. Manninen, R. M. Nieminen, and M. J. Puska, Phys. Rev. B **33**, 4289 (1986).

[22]G. F. Bertsch and D. Tománek, Phys. Rev. B **40**, 2749 (1989).

[23]D. Pines, *Elementary Excitations in Solids* (Benjamin, New York, 1981).

[24]K. Sturm, Z. Phys. B **28**, 1 (1977).

[25]C. Yannouleas, R. A. Broglia, M. Brack, and P. F. Bortignon, Phys. Rev. Lett. **63**, 255 (1989).

[26]R. G. Newton, *Scattering Theory of Waves and Particles* (Springer-Verlag, New York, 1982).

[27]H.-D. Meyer, Phys. Rev. A **34**, 1797 (1986).

[28]We modified the expression for $U^{M}_{L}(\xi,\xi')$ in Ref. 13 by taking the phases for $P^{|M|}_{L}(\xi)$ and $Q^{|M|}_{L}(\xi)$, in accordance to the definitions in Ref. 15.

[29]A. Messiah, *Mécanique Quantique* (Dunod, Paris, 1965), Vol. II.